NUMERICAL STUDY OF THE EFFECT OF GEOMETRY AND BOUNDARY CONDITIONS ON THE COLLAPSE BEHAVIOUR OF STOCKY STIFFENED PANELS

(DOI No: 10.3940/rina.ijme.2012.a2.221)

M C Xu and **C Guedes Soares**, Centre for Marine Technology & Eng., Instituto Superior Tecnico, Portugal

SUMMARY

This study aims at studying different configurations of the stiffened panels in order to identify robust configurations that would not be much sensitive to the imprecision in boundary conditions that can exist in experimental set ups. A numerical study is conducted to analyze the influence of the stiffener's geometry and boundary conditions on the ultimate strength of stiffened panels under uniaxial compression. The stiffened panels with different combinations of mechanical material properties and geometric configurations are considered. The four types of stiffened panels analysed are made of mild or high tensile steel and have bar, 'L' and 'U' stiffeners. To understand the effect of finite element modelling on the ultimate strength of the stiffened panels, four types of FE models are investigated in FE analysis including 3 bays, 1/2+1+1/2 bays, 1+1 bays and 1 bay with different boundary conditions.

NOMENCLATURE

β	Plate slenderness
λ	Column slenderness
a	Length of plate (mm)
b	Width of plate (mm)
B_0	Width of stiffened panels (mm)
t_p	Thickness of plate (mm)
r	Radii of gyration
Φ_p	Effective width of plate elements
S_{yp} , σ_{yp}	Yield stress of plate (MPa)
S_u	Ultimate strength of panels (MPa)
σ_E	Column's Euler stress (MPa)
S_Y , σ_y	Yield stress (MPa)
P_x	Pressure

1. INTRODUCTION

Stiffened panels are very popular structural elements in marine structures and their load carrying capacity is important from the viewpoint of safety and economy. The ratio of strength to weight is an important index to design economical and efficient ship and thus, the thinner plates with high strength steels are adopted. However, thinner plating raises important concerns about the buckling strength.

FE codes have been used to analyse the stress distributions and deformations of very complicated structures with the accuracy demanded in engineering applications under all kinds of loading conditions. They are a suitable tool for assessing the ultimate strength of ship structures. The advanced buckling analysis method is to be based on nonlinear analysis techniques or equivalent, which predict the complex behaviour of stiffened and unstiffened panels [1]. Namely, the extent of the model used in the buckling assessment is to be sufficient to account for the structure that is surrounding the panel of interest, and to reduce the uncertainties introduced through the boundary conditions. In general, the model is to include more than one stiffener span in the stiffener direction and the portion between two primary support members in the transverse direction to the stiffeners.

Boundary conditions affect the ultimate strength of plates [2, 3] and to prescribe appropriate boundary conditions is a main challenge in modelling plates and stiffened panels in experiments and in finite element calculations. Because the boundary of stiffened panels is supported by strong members such as longitudinal girders and transverse frames, the restrained boundary condition is often adopted. But the degree of rotational restraints at the panel boundary is not equivalent to zero. It is important to model the panel edge condition in a relevant way. In order to reproduce adequately the working conditions on ship structures in experimental and numerical models, some of the more important problems are the definition of the boundary conditions on the loaded top edges and unloaded lateral edges of the plate or panel, the control and measurement of out-of-plane eccentricity of the load and the continuity of loads and moments in the panels.

The combined load is very common situation in realistic ship structures and results are available for transverse compression [4], lateral pressure [5] and even combined effects [6]. It is also very important to use experimental results to calibrate the numerical analysis. However, before the combined load condition is considered, the uniaxial compression tests considered here are an initial step that needs to be performed. The three bays longitudinally panels are used instead of single-bay panels in order to properly account for the effect of adjacent plates in the strength of the central one and to avoid boundary conditions problems for the central plates related to eccentricity of load, which was found to be significant by Luís et al. [7, 8].

Some studies have already been performed for stiffened panels. A series of nonlinear finite element method computations were carried out for two full bays (1+1 bays) model with various parameters of influence to investigate the ultimate strength of stiffened panels representative of ship hulls [9]. Zhang & Khan [10] and Fujikubo [11] analysed the ultimate strength of plates using non-linear FE software by one full bay plus two half bays (1/2+1+1/2 bays) model.

Gordo and Guedes Soares [12] conducted an experimental study that was aimed at comparing a new shape of U stiffeners to be used in very fast ships made of ultra-high strength steels (H690) with panels reinforced by the usual shapes of stiffeners. The base geometry is the one used on the tests of Gordo and Guedes Soares [12, 13].

This study aims at studying different configurations of the stiffened panels than the ones in those tests [12], but with the same dimensions of plate fields and stiffeners, in order to decide if there would be more robust configurations that would be less sensitive to the imprecision in boundary conditions that can exist in experimental set ups. The ultimate strength of stiffened panels under axial compression until collapse and beyond are calculated for 120 configurations with different boundary conditions and model geometries. These stiffened panel models include 3 bays, 1/2+1+1/2 bays, 1+1 bays and 1 bay. In the longitudinal direction, the 3 bays model consists of three full bays, the 1/2+1+1/2 bays model consists of one full bay plus two half bays, the 1+1 bays model consists of two full bays, the 1 bay model consists of one full bay. The plate is always high strength steel (S690) but the stiffeners are made of mild or high tensile steel for bar stiffeners and mild steel for 'L' and 'U' stiffeners.

2. DESCRIPTION OF THE MODELS FOR THE ANALYSIS

Figures 1 - 3 show the geometry of the different stiffened panels. Four series of stiffeners are carried out using different types of steel as follows:

- FS series - fully S690 structure: S690 on plating and bar stiffeners.
- BS series - hybrid bar structure: S690 on plating and mild steel on bar stiffeners.
- LS series - hybrid L structure: S690 on plating and mild steel on L stiffeners.
- US series - hybrid U structure: S690 on plating and mild steel on U stiffeners.

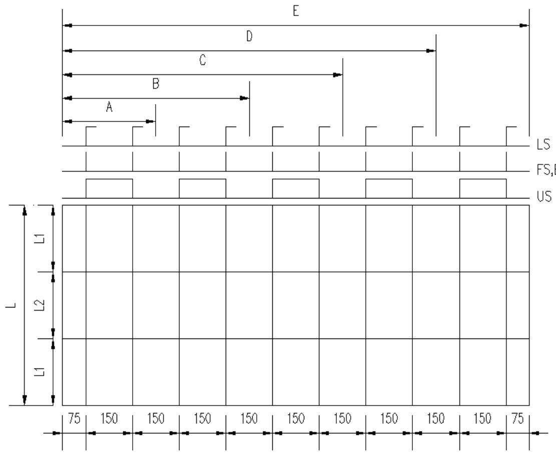

Figure 1 Geometry of 1/2+1+1/2 (L_1=0.5L_2) and 3 bays (L_1=L_2)

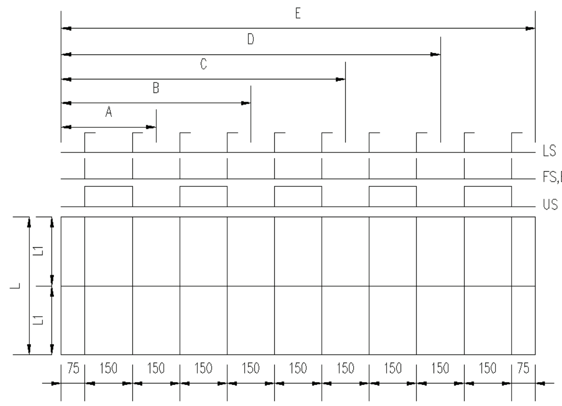

Figure 2 Geometry of 1+1 bays

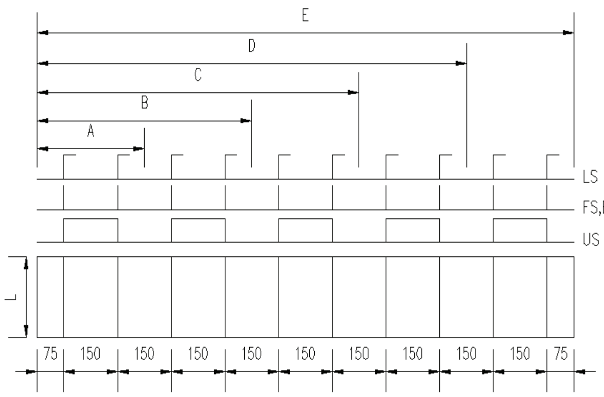

Figure 3 Geometry of 1 bay

Table 1 shows the geometry and material of the stiffened panels, in which the value of I and i are as following: i=1 when I=A, i=2 when I=B, i=3 when I=C, i=4 when I=D, i=5 when I=E. The dimension of the transverse frames is L bar stiffener 50 ×20×6 mm and the thickness of the plates is 4 mm. The A-E means different number of the stiffeners in Figure 1-3, and the FE model of the FS series for three bays is shown in Figure 4. The principal parameters affecting ultimate strength of plate and stiffened panels subjected to compressive load are the plate and column slenderness. The plate slenderness is the same for all plates and it is defined as:

$$\beta = \frac{b}{t_p}\sqrt{\frac{\sigma_{yp}}{E}} \tag{1}$$

The effective width of plate elements (Φ_p) is calculated as [14]:

$$\Phi_p = \frac{2}{\beta} - \frac{1}{\beta^2} \tag{2}$$

The column's Euler stress is evaluated considering the whole plating as effective for the calculation the radii of gyration and is given by

$$\sigma_E = \frac{\pi^2 r^2 E}{L^2} \tag{3}$$

The column slenderness is defined as

$$\lambda = \frac{L}{r}\sqrt{\frac{\sigma_y}{E}} \tag{4}$$

Radii of gyration is: $$r = \frac{I}{A} \tag{5}$$

The application of the concept of column slenderness raises several difficulties when applied to hybrid panels. For the hybrid panels, the yield stress to be used in Eq. (4) σ_Y may be the yield stress of the plating, of the stiffener or the equivalent yield stress. The use of each one leads to completely different results and thus, only the values of $\frac{L}{r}$ and σ_E are presented in Table 2.

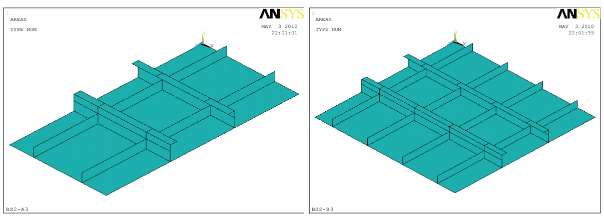

(a) FS2-A3 (b) FS2-B3

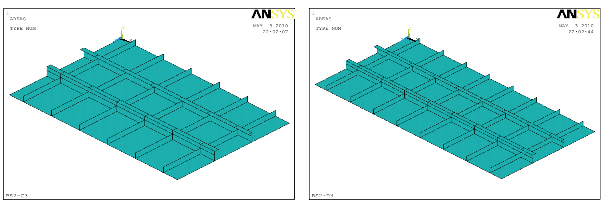

(c) FS2-C3 (d) FS2-D3

Figure 4 FE model of FS series for 3 bays

Table 1 Geometry and material of the stiffened panels

Sample	Plate Dim(mm)	S_Y
FS2-I3	(300×i)×(200×3)×4	
FS2-I21	(300×i)×(100+200+100)×4	
FS2-I22	(300×i)×(200+200)×4	
FS2-I1	(300×i)×200×4	
BS2-I3	(300×i)×(200×3)×4	
BS2-I21	(300×i)×(100+200+100)×4	
BS2-I22	(300×i)×(200+200)×4	
BS2-I1	(300×i)×200×4	690
LS2-I3	(300×i)×(200×3)×4	
LS2-I21	(300×i)×(100+200+100)×4	
LS2-I22	(300×i)×(200+200)×4	
LS2-I1	(300×i)×200×4	
US2-I3	(300×i)×(200×3)×4	
US2-I21	(300×i)×(100+200+100)×4	
US2-I22	(300×i)×(200+200)×4	
US2-I1	(300×i)×200×4	
-	Stiffener Dim(mm)	S_Y
FS2-I3	I 20×4	690
FS2-I21	I 20×4	690
FS2-I22	I 20×4	690
FS2-I1	I 20×4	690
BS2-I3	I 30×8	343
BS2-I21	I 30×8	343
BS2-I22	I 30×8	343
BS2-I1	I 30×8	343
LS2-I3	L38×19×4	296
LS2-I21	L38×19×4	296
LS2-I22	L38×19×4	296
LS2-I1	L38×19×4	296
US2-I3	U (40×150×40) ×2	200
US2-I21	U (40×150×40) ×2	200
US2-I22	U (40×150×40) ×2	200
US2-I1	U (40×150×40) ×2	200

Table 2 Mechanical characteristics of the panels

-	FS	BS	LS	US
β		2.2		
Φ_p		0.702		
L/r	51.7	26	13.9	1.6
σ_E (Mpa)	738	2911	10195	14648

3. NONLINEAR FINITE ELEMENT ANALYSIS

3.1 INTRODUCTION

To investigate the influence of different geometries, 3 bays, 1/2+1+1/2 bays, 1+1 bays and 1 bay stiffened panel with different boundary conditions are simulated in the FE analyses. The FE code 'ANSYS' is used to assess the ultimate strength of the stiffened panels. The shell 181 element is adopted to model the stiffened panels, which is a four nodes element with six degrees of freedom at each node and can account for linear, large rotation and large strain nonlinear. Both full and reduced integration schemes are supported. This element is suitable for analyzing thin-walled structures.

The residual stresses are not included in the FE analyses. The geometric and material nonlinearities are both taken into account, including elastic-plastic large deflection. The assumed material properties use the characteristic values of yield stress and Young's modulus. Where appropriate, a bi-linear isotropic elastic-plastic material model excluding strain rate effects is to be used. A plastic tangent modulus of 1,000 MPa is acceptable for normal and high strength steel [1]. The following are the other material properties: Young's modulus E = 200 GPa and Poisson's ratio v= 0.3.

3.2 BOUNDARY CONDITIONS AND LOADING

The coordinate system and load in the FE analyses is shown in Figure 5.

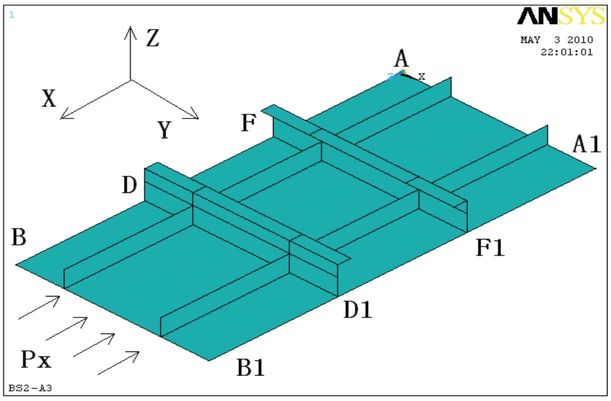

Figure 5 Coordinate system and load in the FE analyses

Table 3 Boundary conditions in the FE analyses

N_{BC}	3 bays			2 bays			2 bays (1+1)		1bay
	C_1	C_2	C_3	C_4	C_5	C_6	C_7	C_8	C_9
1	√	√	√	×	√	×	√	×	×
2	×	×	×	√	×	√	×	√	√
3	√	√	√	×	√	×	√	×	×
4	×	×	×	√	×	√	×	√	√
5	√	√	√	√	√	√	×	×	×
6	×	×	×	×	×	×	√	√	×
7	×	√	√	√	√	√	√	√	×
8	×	×	√	√	√	√	√	√	√
9	×	×	√	√	√	√	√	√	√

Note: Different models and boundary conditions correspond to different location of the stiffeners.

The stiffened panel models, including 3 bays, 1/2+1+1/2 bays, 1+1 bays and 1 bay, are simulated with different boundary conditions as shown in Table 3 and 4. The N_{BC} is the number of the boundary conditions description. To investigate the effect of model geometry and boundary condition on the collapse behaviour of the stiffened panels, nine configurations are calculated in the FE analysis. The pressure Px in the x direction is applied on the edge of the plate and the stiffeners.

Table 4 Description for the boundary conditions

N_{BC}	Description
1	$A\text{-}A_1$:u_x, u_y, u_z, θ_x, θ_y and θ_z
2	$A\text{-}A_1$: u_x, u_y, u_z
3	$B\text{-}B_1$: u_y, u_z, θ_x, θ_y, θ_z and equal u_x
4	$B\text{-}B_1$: u_y, u_z, and equal u_x
5	F, F_1, D, and D_1 on frame (for 3 and 1/2+1+1/2 bays model): u_z
6	F, F_1 on frame (for 1+1 bays model): u_z
7	The intersection between frame and plate: u_z
8	AB edge: u_x, θ_z and θ_x
9	A_1B_1 edge: θ_z, θ_x and equal u_x

3.3 SENSITIVITY ANALYSIS OF ELEMENT SIZE DEFINITION

It has been realized that the incorrect modelling techniques in FE analysis may cause a significant amount of computational errors. The shell elements mesh should be fine enough to properly describe the model shape, also after deformation. A balance between required accuracy and efforts is needed. The FS2-A21 stiffened panel with C_1 condition is used to study the convergence of the mesh sizes in the plate and web of the stiffeners.

Table 5 Ultimate strengths (N_s=5)

No.	N_t	N_l	S_u (MPa)
1	2	4	480
2	4	8	460
3	8	16	455
4	12	24	454
5	16	32	455

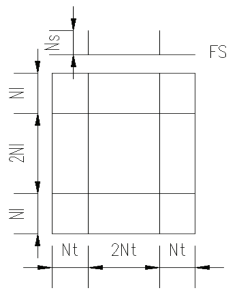

Figure 6 Element setting

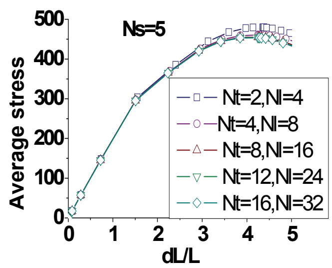

Figure 7 Average stress-shortening curves

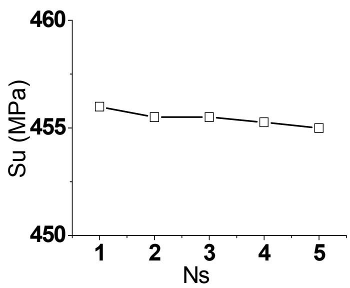

Figure 8 N_s - ultimate strength (S_u)

Figure 6 shows element number setting for N_t, N_l and Ns. Figure 7 and Table 5 shows the average stress-shortening curves and the ultimate strength of the stiffened panel FS2-A21 with different N_t and N_l when N_s is equal to 5. It can be seen that the S_{u3} and S_{u4} are almost the same, namely the mesh size setting as N_t=8 and N_l=16 for the plates is fine enough. Figure 8 show the ultimate strength of the stiffened panel with different N_s, which illustrates that the N_s affect slightly the ultimate strength. According to the mesh sizes convergence study, the mesh sizes are set as N_t=8, N_l=16, Ns=5 and 3 elements in the flange of the frame.

3.4 INITIAL IMPERFECTIONS

It has generally been found that initial imperfections tend to decrease the rigidity and ultimate strength of plates. These initial imperfections affect significantly the ultimate strength of stiffened panel and should be accounted for. The imperfections are caused during a complex fabrication process and are subject to significant uncertainty related to the magnitude and spatial variation.

Kmiecik [15] modelled the initial deflection as the superimposition of the Fourier components. The behaviour of plates subjected to buckling loads depends to a considerable degree on the shape of their initial deflection [16-19]. The most accurate method is to use real measured data, but it is not always available. For design purposes some sort of representative initial imperfection is used [20, 21]. The numerical analysis in this paper aims to investigate the influence of the boundary condition and geometric model on the ultimate strength and thus, the equivalent initial imperfections are assumed as plate initial deflection, column-type initial distortions of stiffeners and sideways initial distortions of stiffeners as follows [22] :

- Hungry horse mode initial deflection (w_{opl}) of the local plate with the shape corresponding to buckling mode due to uniaxial compressive load having the magnitude of b/200.

- Column-type initial deflection (w_{oc}) of the stiffeners with the shape corresponding to buckling mode due to uniaxial compressive load having the magnitude of a/1000.

- Side-ways initial deflection (v_{os}) of the stiffeners with the shape corresponding to buckling mode due to uniaxial compressive load having the magnitude of a/1000.

To impose the initial imperfection in the FE analysis, linear buckling analysis is performed for the target stiffened panel to find out the related buckling modes of the plate and the stiffeners. The geometry properties, for example the thickness of the plates and the stiffeners, are changed to decouple those deformations from lower eigenmodes and to obtain the desired shapes for the plate and the stiffener out-of-plane deformations. The three types of distortions are superimposed altogether in the FE model as equivalent initial imperfection of the stiffened panels.

4. RESULTS OF THE FEM ANALYSIS

The strength of each panel is obtained by summing the reaction force on each node on the opposite boundary where the load is applied and divided by the sectional area of the stiffened panel. These calculations must be performed for each step of the non-linear analysis.

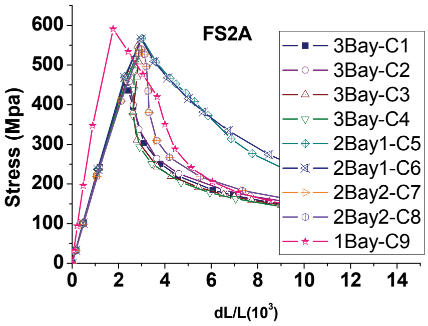

Figure 9 Average stress-shortening curves for FS2-A

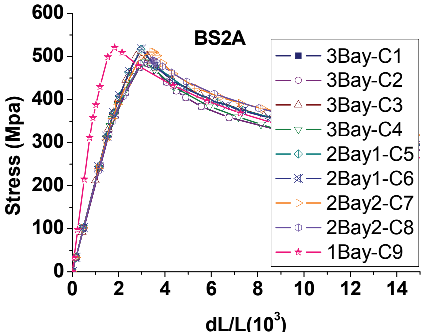

Figure 10 Average stress-shortening curves for BS2-A

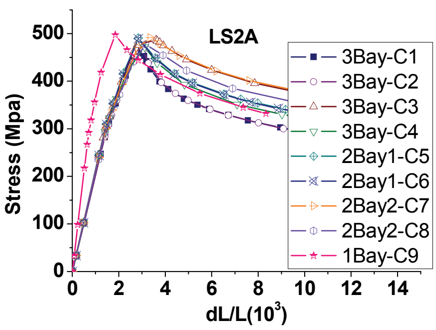

Figure 11 Average stress-shortening curves for LS2-A

Figure 9 - 12 show the average stress-shortening curves of the stiffened panels with B_0 = 300 mm for different models and boundary conditions. It can be seen that a linear behaviour for the FS2-A panels and nonlinear behaviour for the LS2-A, BS2-A and US2-A panels until the ultimate compressive stress are achieved. This main

reason might that the stiffeners suffer lateral buckling and then induce panel failure for the FS2-A panels, which are classified as column failure as shown in Figure 13 and 14. The plate and the stiffeners collapse as a unit, which is needed to avoid by strong the stiffeners. For the LS2-A, BS2-A and US2-A panels, the plates occur buckling, and then induce stiffeners failure. Their collapse modes are plate-induced failure mode.

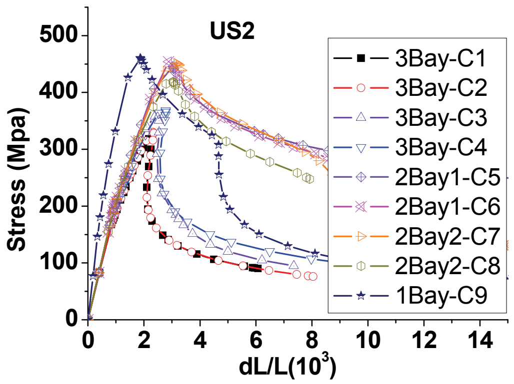

Figure 12 Average stress-shortening curves for US2-A

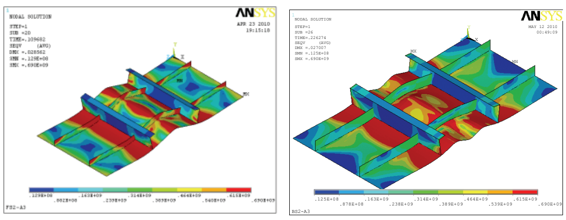

(a) FS2-A (b) BS2-A

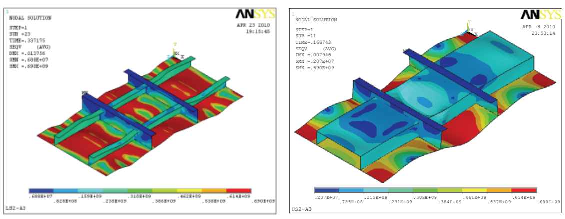

(a) LS2-A (b) US2-A

Figure 13 Equivalent stresses after collapse for C_3

The slopes of average stress-shortening curves during loading are similar in the FE analyses except 1bay-C_9. The boundary condition affects both the collapse behaviours and the ultimate strength. However, this influence depends on the stiffener type to some degree. For the FS2-A panels, the average stress-shortening curves during unloading for the C_5 and C_6 condition are similar for the 1/2+1+1/2 bays model, but drop more slowly than the other cases. For the BS2-A and LS2-A panels, the average stress-shortening curves during unloading are similar between different configurations. For the US2-A panels, the average stress-shortening curves during unloading are similar for the C_5, C_6, C_7 and C_8 configurations, but drop more slowly than the other 3 bays model configurations.

For the stiffened panels under consideration, the FS and US series is more sensitive than the BS and LS series to the boundary condition and the geometric model during unloading. The external one side bay in the 3 bays model supply more flexible constraint for the middle bay than external half side bay in the 1/2+1+1/2 bays model. This causes the different equivalent stress between the 3 and 1/2+1+1/2 bays model as shown in Figure 13 and 14.

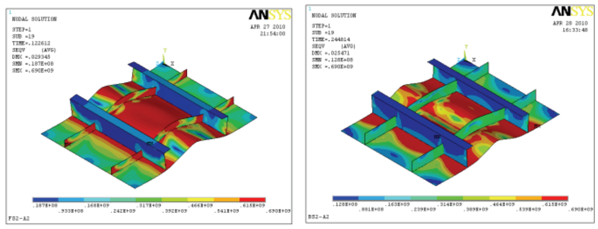

(a) FS2-A (b) BS2-A

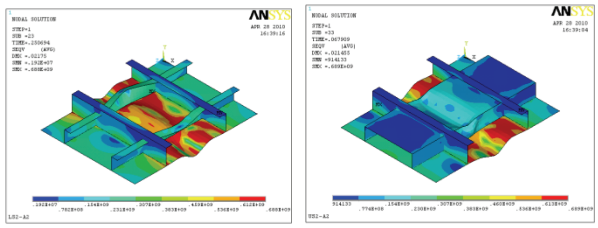

(a) LS2-A (b) US2-A

Figure 14 Equivalent stresses after collapse for C_5

Table 6 Ultimate strengths for the three bays model (MPa)

Case	C_1	C_2	C_3	C_4
FS2-A	455	475	549	517
FS2-B	427	505	546	514
FS2-C	452	515	545	515
FS2-D	375	533	545	512
FS2-E	349	539	545	515
BS2-A	484	484	509	486
BS2-B	497	505	509	487
BS2-C	466	510	509	487
BS2-D	440	520	508	487
BS2-E	424	514	507	487
LS2-A	465	475	487	472
LS2-B	493	493	489	472
LS2-C	496	470	471	471
LS2-D	496	496	479	471
LS2-E	495	496	492	471
US2-A	399	417	445	426
US2-B	394	445	444	430
US2-C	421	441	443	422
US2-D	412	448	446	422
US2-E	413	447	451	422

Figure 15 shows the ultimate strength of the three bays model with the C_1 condition. From the results shown, increasing the width of the panels, namely the number of the stiffeners or the length of the frames, decreases the ultimate strength of the stiffened panels. The displacement in the z direction of the frame is not equal to zero, as shown in Figures 16, which increases with increasing the B_0. This is caused by the stiffness of the frames. The frame should be included in the FE model of panels instead of constraint when the width of panels is very large or the stiffness of the frame is not strong enough.

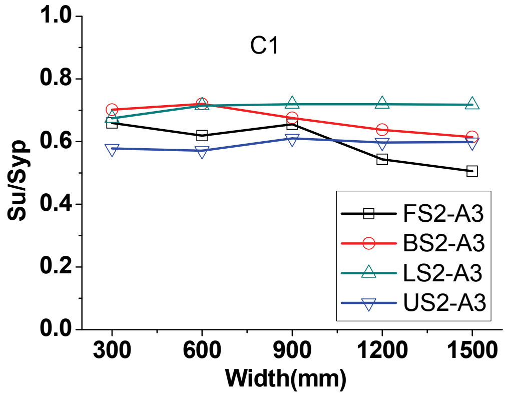

Figure 15 Ultimate strength of three bays model for C_1

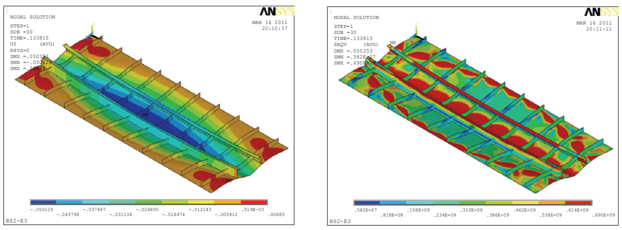

(a) Displacement (b) Equivalent stress
Figure 16 At the ultimate limit state of BS2-E3 for C_1

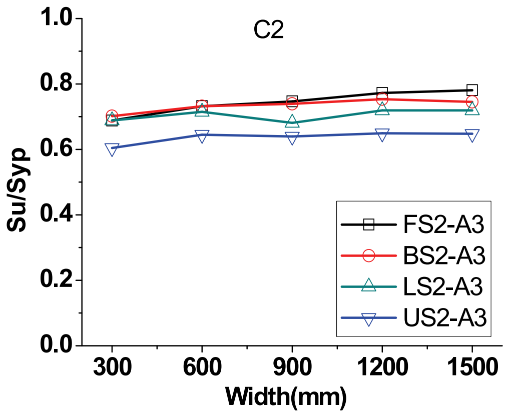

Figure 17 Ultimate strength for 3bays-C_2

The 3bay-C_2 configuration is designed to understand the effect of B_0 on the ultimate strength of the stiffened panels. To ignore the influence of the frame stiffness and to focus on the effectiveness at the lateral plating edges, the displacement in the z direction is constrained between the DD_1 and FF_1 line at the intersection of the plate and the frames for the 3bay-C_2 model. Because the AB and A_1B_1 edges of the panels are totally free to move out-of-plane and to rotate, the ultimate strength increases slowly with increasing width of the panels for the 3bay-C_2 condition as shown in Figure 17. This means that larger panels should be less affected by the lack of effectiveness at the lateral plating edges during buckling. In fact, the percentage of the total cross-section area with reduced effectiveness due to unsupported transverse edges for the wide panels is lower than for the narrow ones and thus, the expected ultimate load is higher for the wider panels. The ratio of the ultimate strength of B_0=1500 mm to B_0=300 mm is 1.13, 1.06, 1.04 and 1.07 for the FS, BS, LS and US series. The symmetric boundary condition for stiffened panels is difficult to apply in experiments. For narrow panels, the influence by the lack of effectiveness at the lateral plating edges should be noticed for some configurations, such as the different error for the FS series is around 13% at least in this circumstance.

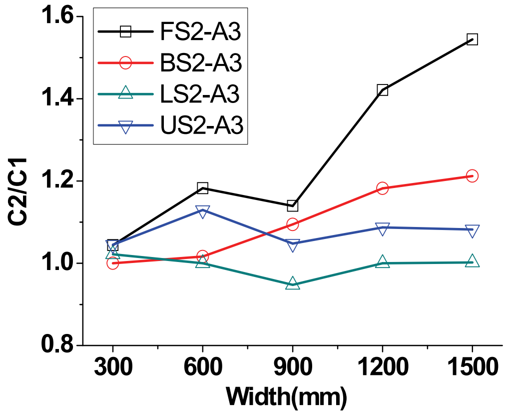

Figure 18 Ratio of the C_2 to C_1 for 3 bays model

Figure 18 shows the ratio of the ultimate strength of the C_2 to C_1. It is observed that the mean value and standard deviation are 1.11 and 0.41 considering all configurations. The ultimate strength in the 3bay-C_2 condition is commonly bigger than that in 3bay-C_1 condition. It would be too optimistic if the displacement in the z direction is constrained at the nodes on the DD_1 and FF_1 line for wide model. The more B_0 increases, the bigger the ratio of the C_2 to C_1 is. The biggest ratio of the C_2 to C_1 for B_0=300 mm and 1500 mm are 1.04 and 1.54. This means that the constraint in the z direction between the DD_1 and FF_1 line is more significantly for wide models than for narrow models. As the panel width grows, the transverse displacement in z direction is increase as the stiffness of the transverse frame decreases due to the constant cross section with longer span. The influence of the constraint in the frame depends on the stiffener type. The difference between the C_2 and C_1 conditions with B_0=1500 mm is 48%, 21%, 2% and 4% for the FS, BS, LS and US series. For the wide panels, the constraint in the z direction on the frame affect significantly the ultimate strength for the FS and BS series, but slightly for the LS and US series.

The symmetric boundary condition is applied on the AB and A_1B_1 edges of the stiffened panels for the C_3 and C_4 condition. This avoids the transverse plating edges to move out-of-plane and to rotate. The magnitude of the ultimate strength is almost the same with increasing the

B_0 for the C_3 and C_4 condition as shown in Figure 19. This illustrates that the width of the panels B_0 affect slightly the ultimate strength of the stiffened panels when symmetric boundary condition is applied on the AB and A_1B_1 edges in the transverse direction. Hence, the narrow model A with the C_3 and C_4 condition for three bays can reduce the influence by the lack of the effectiveness in lateral plating edges. The mean value of the ratio of the C_4 to C_3 is 0.96 which means the ultimate strength is close between the clamped and restrained boundary condition at the end of panels in the longitudinal direction.

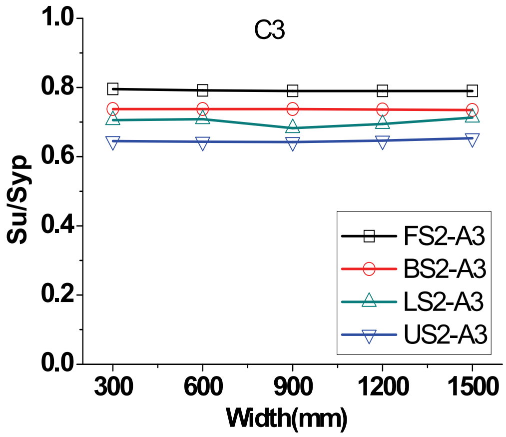

Figure 19 Ultimate strength for 3bays-C_3

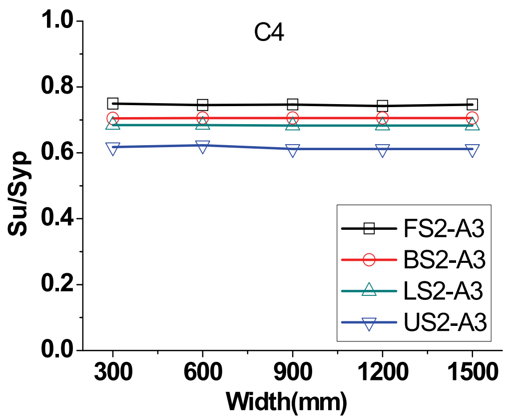

Figure 20 Ultimate strength for 3bays-C_4

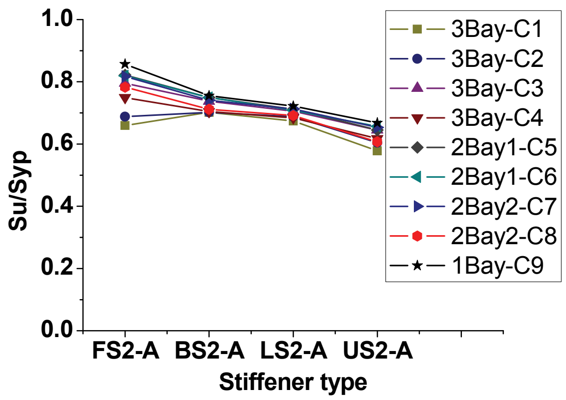

Figure 21 Ultimate strength of the stiffened panels with different configurations (B_0= 300 mm)

Figure 21 presents a comparison of the ultimate strength for different configurations. The ultimate strengths of the stiffened panels with different configurations are different which depends on the stiffener type to some degree. For the stiffened panels under consideration, the FS series is the most sensitive to the boundary condition in the longitudinal direction whose standard deviation is 0.05 for different FE models and boundary conditions in Figure 22. The LS series have the smallest modelling uncertainty whose standard deviation is 0.01. The mean values of the ratio of the C_5 /C_3 and C_6 /C_4 are 1.02 and 1.00 between the 3 and 1/2+1+1/2 bays model, namely the ultimate strength of the 1/2+1+1/2 bays model bigger slightly than the 3 bays model with the same boundary condition. The mean values of the ratio of the C_4/C_3, C_6/C_5 and C_8/C_7 are 0.96, 1.00 and 0.96 respectively. This indicates that the clamped or restrained boundary conditions in the longitudinal direction have only a minor influence on the panel strength.

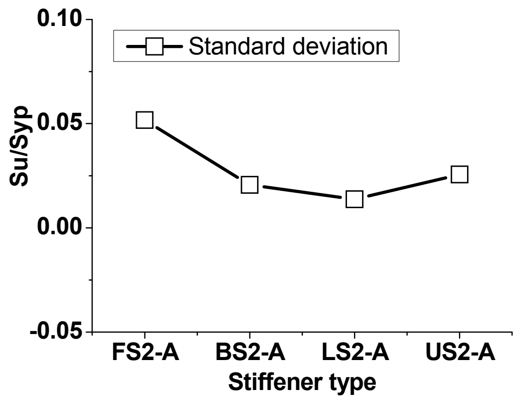

Figure 22 Influence of the stiffener configurations

Figure 23 - 31 show the equivalent stress distributions of the FS series at the ultimate limit state with different configurations for the narrow model A. The collapse shapes of the stiffened panels are different with different FE models and boundary conditions. For the narrow model A, the collapse shapes are similar between the 3bay-C_1 and 3bay-C_2 independently of whether or not the displacement in the z direction on intersection nodes between the plate and the frames is constrained as shown in Figure 23 and 24. It shows that the symmetric boundary condition in the transverse direction affects significantly the collapse shapes in Figure 24 and 25. The collapse modes of the three and 1/2+1+1/2 bays model are similar when their boundary conditions are the same, but their equivalent stress distributions are different in Figure 25 - 28.

The asymmetrical collapse shapes occur for the 1+1 bays model with clamped or restrained boundary condition in the longitudinal direction as shown in Figure 29 and 30. To reduce the uncertainty of modelling for the 1+1 bays model, the periodical symmetric or symmetric boundary condition should be adopted in the longitudinal direction. The collapse shape of the 1 bay model in Figure 31 is different from the other configurations, which cannot consider the interference between adjacent panels and is not recommended. For the 3 bays model, because the constraint of the external side bay with restrained boundary condition is weaker than the middle bay, such as LS2-A3, the external side bays collapse instead of the middle bay as shown in Figure 32. This phenomenon is similar to the experiment, in which there was a premature collapse in the middle part of one of the external spans of the panel due to a non-uniform distribution of load, especially near the contact with the supports [12]. The ultimate average stresses achieved were very low compared to the expected result in the tests. Hence, for the 3 bays model, the loading edges in the longitudinal direction should be constrained strong enough to avoid the external side bay failure before the middle bay collapse in experiment.

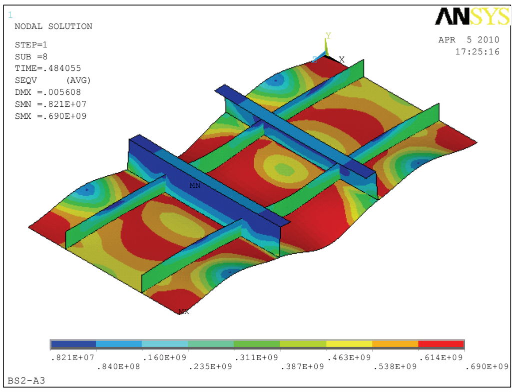

Figure 23 Equivalent stress distributions for 3bay-C_1

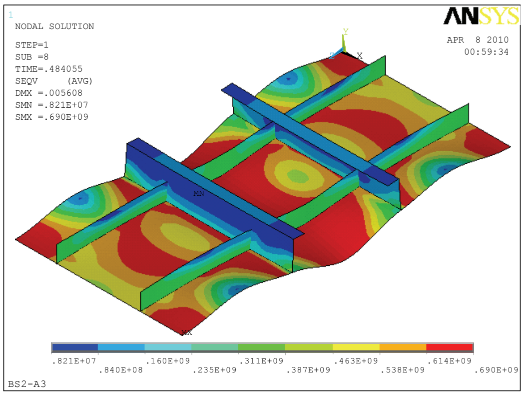

Figure 24 Equivalent stress distributions for 3bay-C_2

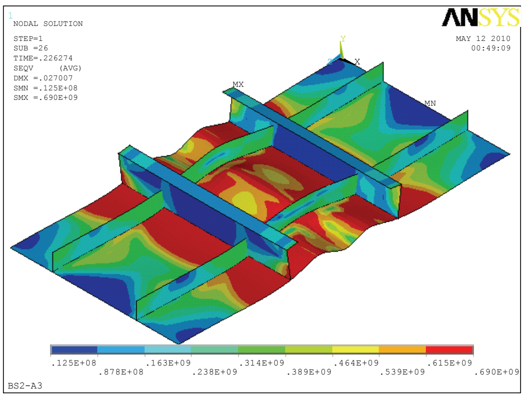

Figure 25 Equivalent stress distributions for 3bay-C_3

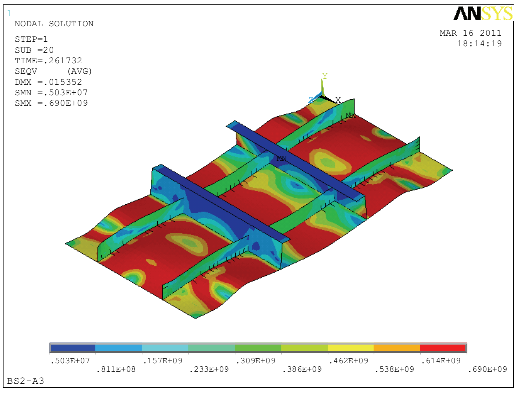

Figure 26 Equivalent stress distributions for 3bay-C_4

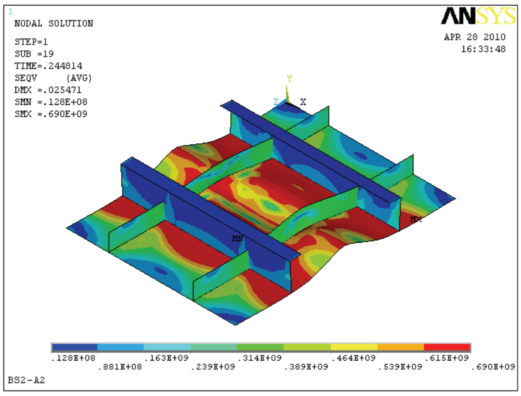

Figure 27 Equivalent stress distributions for 2bay1-C_5

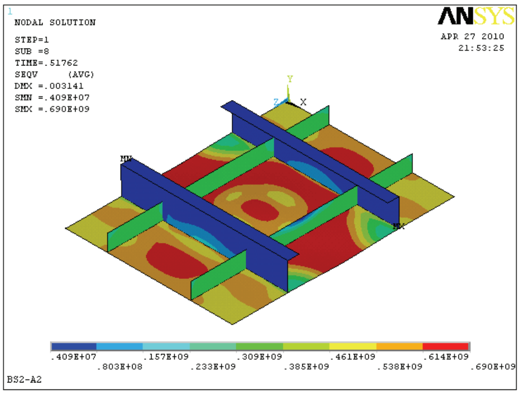

Figure 28 Equivalent stress distributions for 2bay1-C_6

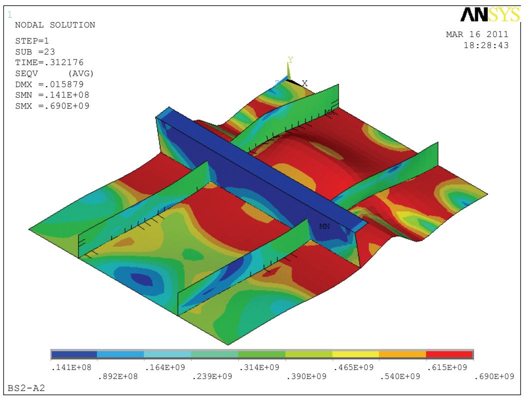

Figure 29 Equivalent stress distributions for 2bay2-C_7

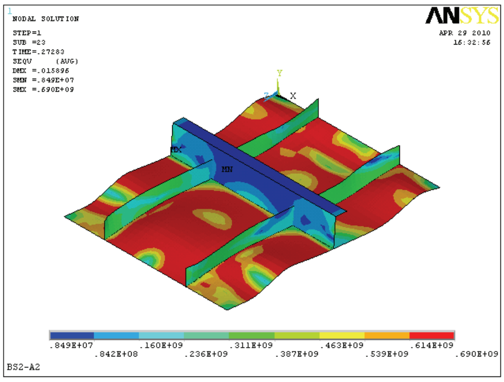

Figure 30 Equivalent stress distributions for 2bay2-C_8

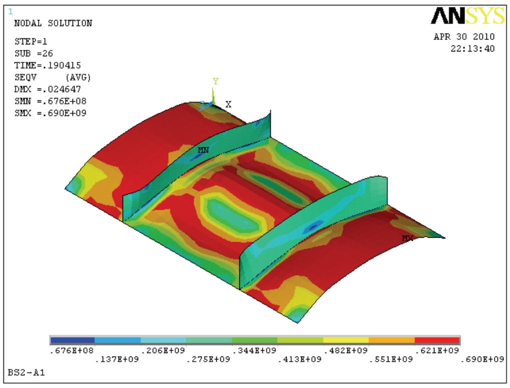

Figure 31 Equivalent stress distributions for 1bay-C_9

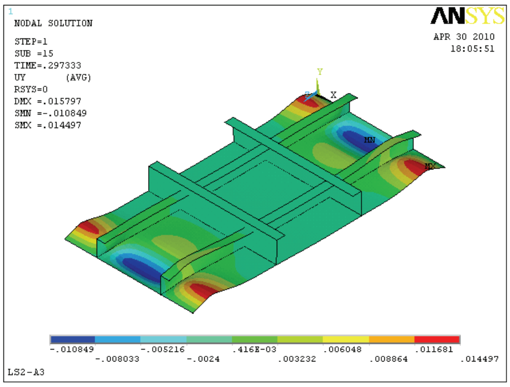

Figure 32 Side bays collapse mode for 3 bays with restrained boundary condition

5. CONCLUSIONS

The boundary conditions and model geometry affect the collapse behaviour and ultimate strength of stiffened panels. This influence depends on the stiffener type in some degree. During loading, the stiffness of the stiffened panels with B_0=300 mm is similar for different configurations except in the C_9 condition. The FS and US series is more sensitive to FE modelling and boundary condition than the BS and LS series.

When the symmetric boundary condition for stiffened panels is not applied at the lateral plate edges, such as in experiments, the influence by the lack of effectiveness at the lateral plating edges should be considered for the FS series whose different error is around 13%. But for the BS, LS and US series, this difference is less than 7%. It would be too optimistic if the displacement in the z direction is constrained at the interaction of the plate and the frames. This influence on wide panels is bigger than narrow panels. For the wide panels, the constraint in the z direction on the frame affect significantly the ultimate strength for the FS and BS series, but slightly for the LS and US series.

The average stress-shortening curves and ultimate strength with 1 bay model is very different from the other configurations which cannot account for the interference between adjacent panels. The asymmetrical collapse modes occur in the 1+1 bays with simply or restraint boundary condition in the longitudinal direction, which would increase the modelling uncertainty [23]. The 1 bay and 1+1 bays models are not recommended in ultimate strength tests of stiffened panels. To reduce the modelling uncertainty for the 1+1 bays model, the periodical symmetric or symmetric boundary condition should be adopted in the longitudinal direction.

The 3 bays and 1/2+1+1/2 bays models allow to have realistic results by avoiding boundary conditions problems for the central plates related to eccentricity of load and including the interference effect between adjacent panels. The ultimate strength of the 1/2+1+1/2 bays model bigger slightly than the 3 bays model with the same boundary condition. The clamped or restrained boundary conditions in the longitudinal direction have only a minor influence on the panel strength. For the 3 bays model with restrained boundary condition, the side bays collapse instead of the middle bay in some case in the FE analyses and the experiment. Hence, the boundary condition for 3 bays model in the longitudinal direction should be strong enough to avoid the side bays collapse instead of the middle bay.

6. ACKNOWLEDGEMENTS

The first author has been financed by the Portuguese Foundation for Science and Technology (Fundação para a Ciência e Tecnologia), under contract SFRH / BD / 65120/ 2009.

7. REFERENCES

1. IACS, 2006. Common Structural Rules for Bulk Carriers. International Association of Classification Societies, London
2. Guedes Soares C., 1988. Design equation for the compressive strength of unstiffened plate elements with initial imperfections. *Journal of Constructional Steel Research* (9), pp. 287-310.
3. Guedes Soares C., Kmiecik M., 1995. Influence of the boundary conditions on the collapse strength of square plates with initial imperfections. Marine Technology and

Transportation Conference, Computational Mechanics Publications, Graczyk, T., Jastrzebski, T., Brebbia C. A. and Burns, R. (Eds.), pp. 227-235.

4. Guedes Soares C., Gordo J. M., 1996. Collapse strength of rectangular plates under transverse compression. *Journal of Constructional Steel Research* 36(3), pp. 215-234.
5. Teixeira A. P., Guedes Soares C., 2001. Strength of compressed rectangular plates subjected to lateral pressure. *Journal of Constructional Steel Research* (57), pp. 491-516.
6. Guedes Soares C., Gordo J. M., 1996. Compressive strength of rectangular plates under biaxial load and the lateral pressure. *Thin-Walled Structures* (24), pp. 231-259.
7. Luís R. M., Guedes Soares C., Nikolov P.I., 2008. Collapse strength of longitudinal plate assemblies with dimple imperfections. *Ships and Offshore Structures* 3(4), pp. 359-370.
8. Luís R.M., Witkowska M., Guedes Soares C., 2008. Ultimate strength of transverse plate assemblies under uniaxial loads. *Journal of Offshore Mechanics and Arctic Engineering* 130(2), pp. 021011(1-7).
9. Paik J.K., Branner K., Choo Y.S., Czujko J., Fujikubo M., Gordo J.M., Parmentier G., Iaccarino R., O'Neil S., Pasqualino I., Wang D., Wang X., Zhang S., 2009. Report of committee III.1: Ultimate Strength, *Proceedings of the 17th International Ship and Offshore Structures Congress* (ISSC 2009), pp. 16-21.
10. Zhang S., Khan I., 2009. Buckling and ultimate capability of plates and stiffened panels in axial compression. *Marine Structures* (22), pp. 791-808.
11. Fujikubo M., Haradab M., Yao T., Khedmatid M.R., Yanagiharaa D., 2005. Estimation of ultimate strength of continuous stiffened panel under combined transverse thrust and lateral pressure Part 2: Continuous stiffened panel. *Marine Structures* (18), pp.411-427.
12. Gordo J.M., Guedes Soares C., 2008. Compressive tests on short continuous panels, *Marine Structures* (21), pp. 113-137.
13. Gordo J.M., Guedes Soares C., 2007. Experimental evaluation of the behaviour of a mild steel box girder under bending moment. In: Guedes Soares, C, Das, P.K., (Eds), *Advancements in Marine Structures,* Taylor and Francis, pp. 377-383.
14. Faulkner D., 1975. A review of effective plating for use in the analysis of stiffened plating in bending and compression. *J. Ship Research* (19), pp.1-7.
15. Kmiecik M., 1970. The load-carrying capacity of axially loaded longitudinally stiffened plate panels having initial deformations, Report No R80, *Ship Research Institute*, Trondheim.
16. Frieze P. A., Dowling P. J., Hobbs R. H., 1977. Ultimate load behaviour of plates in compression, In *Steel Plated Structures*, ed. P. J. Dowling et al. Crosby Lockwood Staples, London, pp. 24-50,.
17. Ueda Y., Yao T., 1985. The influence of complex initial deflection modes on the behaviour and ultimate strength of rectangular plates in compression. *J. Constructional Steel Research* (5), pp.265-302,.
18. Guedes Soares C., Kmiecik M., 1993. Simulation of the ultimate compressive strength of unstiffened rectangular plates, *Marine Structures* (6), pp.553-569.
19. Sadovský Z., Teixeira A. P., Guedes Soares C., 2005. Degradation of the compression strength of rectangular plates due to initial deflection. *Thin-Walled Structures* (43), pp. 65-82.
20. Guedes Soares C., 1992. Design equation for ship plate elements under uniaxial compression. *J. Constructional Steel Research* (22), pp. 99-114.
21. Guedes Soares C., Gordo J.M., 1997. Design methods for stiffened plates under predominantly uniaxial compression, *Marine Structures* (10), pp.465-497.
22. Paik J.K., Seo J.K., 2009. Nonlinear finite element method models for ultimate strength analysis of steel stiffened-plate structures under combined biaxial compression and lateral pressure actions-Part II: Stiffened panels, *Thin-Walled Structures* (47), pp. 998-1007.
23. Guedes Soares C., 1988. Uncertainty modelling in plate buckling. *Structural Safety* (5), pp. 17-34.